

# Spinning-Charged-Hairy Black Holes in 5-d Einstein gravity

Y. Brihaye<sup>a†</sup>, L. Ducobu<sup>b†</sup>

<sup>†</sup>Physique-Mathématique, Université de Mons, Mons, Belgium

July 27, 2018

## Abstract

The spinning-hairy black holes that occur in Einstein gravity supplemented by a doublet of complex scalar fields are constructed within an extension of the model by a  $U(1)$  gauge symmetry involving a massless vector potential. The hairy black holes then acquire an electric charge and a magnetic moment; their domain of existence is discussed in terms of the gauge coupling constant.

## 1 Introduction

One century after the discovery of General Relativity (GR) by Einstein in 1915, the research in this topic has never been so intensive and exciting. This is mainly boosted by two antinomic phenomena: the direct observation of gravitational waves and the desperately lack of evidence of dark matter. For obvious reasons, the main effort is realized essentially in four dimensional space-time but there are numerous reasons to study GR in higher dimensions (see e.g [1] and references therein). Besides looking at our Universe with a String theory or Brane-World point of view, the study of GR in  $d > 4$  dimensions provides an inexhaustible domain of research and a fertile ground for new discoveries and innovating techniques. First the basic Einstein-Hilbert action can be enlarged by a hierarchy of Lovelock actions involving higher powers in the Riemann tensor [2]; the first term of which being the Gauss-Bonnet action. Second, while the basic classical solutions in 4-d gravity are drastically featureless [3] (the electro vacuum black holes being described by a few macroscopic degrees of freedom), higher dimensional gravity admit families of new classical solutions, black holes with horizon topologies other than the sphere [4],[1].

Escaping the rigidity of the “No-hair” conjecture [5] has been a long fight which (up to our knowledge) was broken first time in [6] (see also [7]). Attracting a lot of interest, families of four-dimensional hairy black holes endowed by scalar hairs have been constructed in [8],[9]. The model consists of the standard Einstein gravity minimally coupled to a massive, complex, scalar field. Among ingredients entering crucially in this construction let us point out that: (i) the black hole has to spin sufficiently fast, (ii) the solution is synchronized in the sense that the spinning velocity of the black hole on the horizon coincides with the frequency, say  $\omega$ , parametrizing the harmonic time-dependence of the scalar field, (iii) the solutions bifurcate for a peculiar sub-family of (hairless) Kerr solutions, (iv) the solution involves the numerical integration of a set non-linear partial differential equations.

The discovery of these solutions motivated research of similar solutions in different extensions of the model and/or in different gravity frameworks, see e.g. [10]. Also it is natural to emphasize that hairy black holes exist in higher dimensional gravity extended by an appropriate matter sector. In space-time with odd dimensions the construction of spinning black holes is technically simpler since a suitable ansatz of the metric leads to differential equations (instead of partial derivative ones). As a consequence, some aspects of hairy black holes can be studied in such space-time.

---

<sup>a</sup>yves.brihaye@umons.ac.be

<sup>b</sup>ludovic.ducobu@umons.ac.be

In the absence of matter field, the generic spinning black holes of  $d > 4$  space-time gravity are the Myers-Perry (MP) solutions [11]. Supplementing the Einstein-Hilbert action by a single complex scalar leads essentially to non-spinning boson stars. To our knowledge, no parametrization of the metric and matter functions can be implemented to obtain spinning solutions or black holes. One possible key ingredient for obtaining spinning boson stars and black holes consists in the inclusion of a doublet of complex scalar fields. This has been proposed in [12] for the construction of spinning boson stars in  $d = 5$  and, using a similar ansatz for the scalar fields, spinning black holes in  $d = 5$  gravity were constructed in [13] and [14]. One main feature of these results is that, unlike the  $d = 4$  case, the spinning hairy black holes remain decoupled from the family of MP solutions. Interestingly, the family of  $d = 5$  hairy black holes is “envelopped” by the boson stars on the one side and by a family of extremal solution on the second side. Asymptotically AdS black holes and boson stars were constructed in [15] with the same matter content but with a slightly different parametrization. Similar to the  $d = 4$  case, these black holes bifurcate from the AdS-Myers-Perry solutions.

On the other hand, supplementing gravity by gauge fields often results in families of charged objects (black holes or solitons) presenting new physically interesting properties. The oldest and most famous example is the occurrence of extremal solutions of Reissner-Nordstrom black holes. Recently, it was revealed that charged black holes possess the property of superradiance [16, 17, 18]. The coupling of the  $d=4$  hairy black holes solutions of [8] to electromagnetism has been investigated in details [19].

Recently it was shown [20] that, in  $d=5$ , non-spinning hairy black holes exist in the Einstein-Gauss-Bonnet-Maxwell theory provided both -the gauge coupling constant and the Gauss-Bonnet parameters- are sufficiently large. Several properties of these solutions have been discussed in [21]. To our knowledge, the gauge version of  $d=5$  spinning black holes has not yet been studied and this problem is emphasized in this paper.

The ingredients of the model, the ansatz and the boundary conditions are presented in the second section. In Sect. 3 we review the properties of the non-hairy solutions: the Myers-Perry and Reissner-Nordstrom solutions. For completeness, the uncharged spinning hairy black holes are briefly summarized in Sect. 4 and the new results are presented in Sect. 5. Because of their rotation, the family of black holes in the full model acquire an electric charge as well as a magnetic moment. Finally, in section 6 we summarize our results and conclude.

## 2 The field equations

### 2.1 The model

Following the conventions of [12], we consider the action of the self-interacting complex doublet scalar field  $\Phi$  coupled minimally to Einstein gravity in 5 dimensional spacetime and supplemented by a Maxwell field

$$S = \int \left[ \frac{R}{16\pi G} - (D_\mu \Phi)^\dagger (D^\mu \Phi) - U(|\Phi|) - \frac{1}{4} F_{\mu\nu} F^{\mu\nu} \right] \sqrt{-g} d^5x. \quad (2.1)$$

In the first term,  $R$  represents the curvature scalar and  $G$  the Newton’s constant (in 5 dimensions). The second term is the kinetic part of the scalar field with  $\Phi = (\phi_1, \phi_2)^t$  and  $A^\dagger$  denotes the complex transpose of  $A$ . The third term  $U$  is a self-interaction potential depending on the norm  $|\Phi|^2 = \Phi^\dagger \Phi$ . With this choice, the scalar sector possesses an  $U(2)$  global symmetry whose any  $U(1)$  subgroup can be gauged. In this work, we will gauge the diagonal  $U(1) \times U(1)$  subgroup. Then the covariant derivative and Faraday tensor take the form

$$D_\mu = (\partial_\mu - iqA_\mu \mathbb{I}_2) \quad , \quad F_{\mu\nu} = \partial_\mu A_\nu - \partial_\nu A_\mu,$$

where  $\mathbb{I}_2$  is the  $2 \times 2$  identity matrix, and  $q$  denotes the gauge coupling constant. We will assume  $q > 0$  since the sign of  $q$  can be reabsorbed in the gauge fields.

Variation of the action with respect to the metric leads to the Einstein equations

$$G_{\mu\nu} = R_{\mu\nu} - \frac{1}{2} g_{\mu\nu} R = 8\pi G (T_{\mu\nu}^s + T_{\mu\nu}^v) \quad (2.2)$$

with stress-energy tensor

$$T_{\mu\nu}^s = (D_\mu\Phi)^\dagger(D_\nu\Phi) + (D_\nu\Phi)^\dagger(D_\mu\Phi) - \frac{1}{2}g_{\mu\nu} \left[ (D_\alpha\Phi)^\dagger(D_\beta\Phi) + (D_\beta\Phi)^\dagger(D_\alpha\Phi) \right] g^{\alpha\beta} - g_{\mu\nu}U(|\Phi|), \quad (2.3)$$

$$T_{\mu\nu}^v = F_{\mu\alpha}F_\nu{}^\alpha - \frac{1}{4}g_{\mu\nu}F_{\alpha\beta}F^{\alpha\beta}, \quad (2.4)$$

where the upper-script  $s$  stand for *scalar* while the upper-script  $v$  stand for *vector*, *i.e.* the Maxwell field.

The variation with respect to the matter fields leads respectively to the equations,

$$\frac{1}{\sqrt{-g}}D_\mu(\sqrt{-g}D^\mu\Phi) = \frac{\partial U}{\partial|\Phi|^2}\Phi, \quad \frac{1}{\sqrt{-g}}\partial_\mu\sqrt{-g}F^{\mu\nu} = J^\nu, \quad J^\nu = iq((D^\nu\Phi)^\dagger\Phi - \Phi^\dagger(D^\nu\Phi)). \quad (2.5)$$

## 2.2 The Ansatz

While rotating EKG black holes will generically possess two independent angular momenta and a more general topology of the event horizon we restrict here to configurations with equal-magnitude angular momenta and a spherical horizon topology.

Thus the solutions possess bi-azimuthal symmetry, implying the existence of three commuting Killing vectors,  $\xi = \partial_t$ ,  $\eta_1 = \partial_{\varphi_1}$ , and  $\eta_2 = \partial_{\varphi_2}$ .

A suitable metric ansatz in this case reads

$$ds^2 = \frac{dr^2}{f(r)} + g(r)d\theta^2 + h(r)\sin^2\theta(d\varphi_1 - W(r)dt)^2 + h(r)\cos^2\theta(d\varphi_2 - W(r)dt)^2 + (g(r) - h(r))\sin^2\theta\cos^2\theta(d\varphi_1 - d\varphi_2)^2 - b(r)dt^2, \quad (2.6)$$

where  $\theta \in [0, \pi/2]$ ,  $(\varphi_1, \varphi_2) \in [0, 2\pi]$ , and  $r$  and  $t$  denote the radial and time coordinate, respectively.

For such solutions the isometry group is enhanced from  $\mathbb{R}_t \times U(1)^2$  to  $\mathbb{R}_t \times U(2)$ , where  $\mathbb{R}_t$  denotes the time translation. This symmetry enhancement allows to factorize the angular dependence and thus leads to ordinary differential equations.

Completing the metric (2.6), the scalar field is taken in the form used in [12] :

$$\Phi = F(r)e^{i\omega t} \begin{pmatrix} \sin\theta e^{i\varphi_1} \\ \cos\theta e^{i\varphi_2} \end{pmatrix}, \quad (2.7)$$

where the frequency  $\omega$  parametrized the harmonic time-dependence. For the scalar field potential we restrict our study to the simplest case

$$U(|\Phi|) = \mu^2\Phi^\dagger\Phi = \mu^2F(r)^2 \quad (2.8)$$

where  $\mu$  corresponds to the scalar field mass.

Finally the electromagnetic potential is chosen in the form

$$A_\mu dx^\mu = V(r)dt + A(r)(\sin^2(\theta)d\varphi_1 + \cos^2(\theta)d\varphi_2) \quad (2.9)$$

which turns out to be consistent with the symmetries of the metric and scalar fields. The whole ansatz leads to a consistent set of differential equations for the radial functions  $f, b, h, g, W, V, A$  and  $F$ .

Without fixing a metric gauge, a straightforward computation leads to the following reduced action for the system

$$A_{\text{eff}} = \int drdt L_{\text{eff}}, \quad \text{with} \quad L_{\text{eff}} = L_g + 16\pi G(L_s + L_v), \quad (2.10)$$

with

$$L_g = \sqrt{\frac{fh}{b}} \left( b'g' + \frac{g}{2h}b'h' + \frac{b}{2g}g'^2 + \frac{b}{h}g'h' + \frac{1}{2}ghW'^2 + \frac{2b}{f}\left(4 - \frac{h}{g}\right) \right), \quad (2.11)$$

$$L_s = g\sqrt{\frac{bh}{f}} \left( fF'^2 + \left( \frac{2}{g} + \frac{(1-qA)^2}{h} - \frac{(\omega - W + q(V + WA))^2}{b} + \mu^2 \right) F^2 \right), \quad (2.12)$$

$$L_v = g\sqrt{\frac{bh}{f}} \left( \frac{2A^2}{g^2} + \frac{f}{2h}(A')^2 - \frac{f}{2b}(V' + WA')^2 \right) \quad (2.13)$$

where a prime denotes a derivative with respect to  $r$ .

It can be checked that the full Einstein equations (2.2) are recovered by taking the variation of  $A_{\text{eff}}$  with respect to  $h, b, f, g$  and  $W$ . The Klein-Gordon and Maxwell equations are found by taking the variation with respect to  $F, V$  and  $A$ .

The metric gauge freedom can be fixed afterwards, leading to a system of seven independent equations plus a constraint which is a consequence of the other equations. For the construction of the solutions, we have fixed the metric gauge by taking

$$g(r) = r^2 \quad (2.14)$$

consistently with the standard analytic form of the Myers-Perry solution. Appropriate combinations of the equations can be used in such a way that only the first derivative of  $f$  appears in the system. Accordingly, the equation for  $f(r)$  is a first order equation while the equations of the six other fields are of the second order.

### 2.3 Asymptotics

The submanifold of space-time characterized by a fixed value of the radial and time coordinates,  $r = r_H > 0$  and  $t = t_0$  respectively, is a squashed  $S^3$  sphere. Imposing the horizon of the metric by means of the conditions  $f(r_H) = b(r_H) = 0$  therefore leads to black holes with the same horizon topology.

Restricting to nonextremal solutions, the following expansion holds near the event horizon:

$$\begin{aligned} f(r) &= f_1(r - r_H) + O(r - r_H)^2, & h(r) &= h_H + O(r - r_H), \\ b(r) &= b_1(r - r_H) + O(r - r_H)^2, & w(r) &= \Omega_H + w_1(r - r_H) + O(r - r_H)^2, \\ V(r) &= V_H + V_1(r - r_H) + O(r - r_H)^2, & A(r) &= A_H + V_1(r - r_H) + O(r - r_H)^2, \\ F(r) &= F_0 + F_1(r - r_H) + O(r - r_H)^2. \end{aligned} \quad (2.15)$$

A straightforward calculation gives the following asymptotic expansion for the solution

$$\begin{aligned} b(r) &= 1 + \frac{\mathcal{U}}{r^2} + \dots, & f(r) &= 1 + \frac{\mathcal{U}}{r^2} + \dots, & h(r) &= r^2 + \frac{\mathcal{V}}{r^2} + \dots, & W(r) &= \frac{\mathcal{W}}{r^4} + \dots, \\ V(r) &= V_0 + \frac{q_e}{r^2} + \dots, & A(r) &= \frac{q_m}{r^2} + \dots, & F(r) &= c_0 \frac{e^{-\sqrt{\mu^2 - (\omega - qV_0)^2} r}}{r^{3/2}} + \dots, \end{aligned} \quad (2.16)$$

which guarantees Minkowski spacetime background to be approached at infinity. In this expansion,  $\mathcal{U}, \mathcal{V}, \mathcal{W}, q_e, q_m, V_0$  and  $c_0$  are free parameters that can be reconstructed from the result of the numerical integration on  $[r_H, \infty[$ .

Note that, in the last equation (2.16), one can see that the scalar field acquires a squared effective mass  $M_{\text{eff}}^2 = \mu^2 - (\omega - qV_0)^2$ . The condition

$$\mu - |\omega - qV_0| > 0 \quad (2.17)$$

should therefore be obeyed to guarantee bound-state (or localized) solutions.

This condition generalizes the bound-state condition known for uncharged solutions : that is  $\omega < \mu$ , see fig. 1 (where we put  $\mu = 1$  without loss of generality).

## 2.4 Boundary conditions

We will not write explicitly the field equations which are lengthy and non illuminating. However, one can easily see from (2.12) that the regularity of the solutions at the horizon implies a generalized synchronization condition between the frequency  $\omega$  of the scalar field and the rotation velocity  $\Omega_H \equiv W(r_H)$  of the black hole at the horizon

$$\omega - \Omega_H + q(V_H + A_H\Omega_H) = 0.$$

This condition can be used to determine the frequency  $\omega$  in terms of the other parameters.

Because the electric potential  $V(r)$  can be shifted up to a redefinition of quantity  $A_H\Omega_H$  and the frequency  $\omega$ , we will take advantage of this freedom to set  $V_H = 0$ . The condition would then become

$$\omega - \Omega_H + qA_H\Omega_H = 0. \quad (2.18)$$

This condition generalizes the so called ‘‘synchronisation condition’’ ( $\omega = \Omega_H$ ) known for the uncharged case. We clearly see here that, for a given value of  $\Omega_H \neq 0$ , the synchronisation condition holds **iff**  $q = 0$  or  $A_H = 0$ .

The regularity of the equations for the fields  $h(r)$ ,  $W(r)$  and the Maxwell equations imply three independent non trivial conditions to be obeyed at the horizon, we will note them symbolically  $\Gamma_h, \Gamma_W, \Gamma_V$ ; these are lengthy polynomials in the various fields and their first derivative, we do not write them explicitly because they are not illuminating. Summarizing, we have eight conditions at the horizon

$$f(r_H) = 0, \quad b(r_H) = 0, \quad W(r_H) = \Omega_H, \quad V(r_H) = 0, \quad A(r_H) = A_H, \quad \Gamma_{h,W,V} = 0. \quad (2.19)$$

where  $A_H$  is an undetermined constant.

The boundary value problem is then fully specified by imposing the conditions (2.19) at the horizon and the asymptotic conditions (2.16) for  $b, h, W, A$  and  $F$ .

## 2.5 Rescaling

The theory is determined by three parameters :  $G, \mu, q$ . The constants  $G$  and  $\mu$  can be rescaled into the matter fields and the radial variable. We will use rescaled quantities such that  $\mu = 1$  and  $8\pi G = 1$ . The gauge coupling  $q$  is therefore the only intrinsic parameter of the model.

The hairy black holes will be specified by the event horizon radius  $r_H$ , the horizon velocity  $\Omega_H$  and the value  $A_H$ .

The (constant) horizon angular velocity  $\Omega_H$  is defined in terms of the Killing vector  $\chi = \partial/\partial t + \Omega_1\partial/\partial\varphi_1 + \Omega_2\partial/\partial\varphi_2$  which is null at the horizon. For the solutions within the ansatz (2.6), the horizon angular velocities are equal,  $\Omega_1 = \Omega_2 = \Omega_H$ .

## 2.6 Quantities of interest

The mass and angular momentum of the solutions are given by

$$M = -\frac{3S_3}{16\pi G}\mathcal{U}, \quad J = \frac{S_3}{8\pi G}\mathcal{W}, \quad (2.20)$$

where  $S_3 = 2\pi^2$  denotes the area of the unit three-dimensional sphere.

The solution is further characterized by the electric charge  $Q_e$  and magnetic moment  $Q_m$ , these quantities are related to the parameters  $q_e$  and  $q_m$  by

$$Q_e = \frac{2S_3}{4\pi G}q_e, \quad Q_m = \frac{2S_3\pi^2}{4\pi G}q_m. \quad (2.21)$$

Finally the gyromagnetic ratio  $\tilde{g}$  can be computed :  $\tilde{g} = 2MQ_m/(Q_eJ)$ . Other quantities of interest are the Hawking temperature  $T_H$  and the area  $\mathcal{A}_H$  of the black hole horizon

$$T_H = \frac{\sqrt{b_1 f_1}}{4\pi}, \quad \mathcal{A}_H = \sqrt{h_H r_H^2} S_3. \quad (2.22)$$

The horizon mass and angular momentum  $M_H, J_H$  can further be defined (see e.g. [22]); these quantities obey a Smarr relation of the form

$$M_H = \frac{3}{2} \left( \frac{\mathcal{A}_H T_H}{4} + 2\Omega_H J_H \right). \quad (2.23)$$

This has been used as a numerical test of our numerical results.

In order to figure out the way the distribution of the energy of the scalar field is affected by the electromagnetic field, we will present the energy density of some solutions. For completeness, we write these formulas

$$\begin{aligned} \mathcal{E}_v &= g \sqrt{\frac{bh}{f}} \left( \frac{f}{2bh} (A')^2 (b - hW^2) + \frac{2}{g^2} A^2 + \frac{f}{2b} (V')^2 \right), \\ \mathcal{E}_s &= g \sqrt{\frac{bh}{f}} \left( f(F')^2 + \mu^2 F^2 + F^2 \left( \frac{2}{g} + \frac{(1 - qA)^2}{h} \right) + \frac{F^2}{b} [(qV - \omega)^2 - W^2(qA - 1)^2] \right). \end{aligned}$$

### 3 Non-hairy solutions

In the absence of the scalar field ( $\Phi = 0$ ), two types of solutions exist that are known in analytic form.

#### 3.1 Uncharged, spinning black holes

In the absence of the Maxwell field one recovers the MP (vacuum) black holes [11] with equal-magnitude angular momenta. Expressed in terms of the event horizon radius and the horizon angular velocity<sup>1</sup> (which are the control parameters in our numerical approach), this solution reads

$$\begin{aligned} f(r) &= 1 - \frac{1}{1 - r_H^2 \Omega_H^2} \left( \frac{r_H}{r} \right)^2 + \frac{r_H^2 \Omega_H^2}{1 - r_H^2 \Omega_H^2} \left( \frac{r_H}{r} \right)^4, \quad h(r) = r^2 \left( 1 + \left( \frac{r_H}{r} \right)^4 \frac{r_H^2 \Omega_H^2}{1 - r_H^2 \Omega_H^2} \right), \\ b(r) &= 1 - \left( \frac{r_H}{r} \right)^2 \frac{1}{1 - (1 - (\frac{r_H}{r})^4) r_H^2 \Omega_H^2}, \quad W(r) = \left( \frac{r_H}{r} \right)^4 \frac{\Omega_H}{1 - (1 - (\frac{r_H}{r})^4) r_H^2 \Omega_H^2}. \end{aligned} \quad (3.24)$$

Therefore, for a MP black hole, the relevant parameters in the event horizon expansion (2.15) are

$$f_1 = \frac{2(1 - 2r_H^2 \Omega_H^2)}{r_H(1 - r_H^2 \Omega_H^2)}, \quad b_1 = \frac{2}{r_H}(1 - 2r_H^2 \Omega_H^2), \quad w_1 = \frac{4\Omega_H}{r_H}(r_H^2 \Omega_H^2 - 1), \quad (3.25)$$

while the constants  $\mathcal{U}$ ,  $\mathcal{V}$  and  $\mathcal{W}$  in the far field expansion (2.16) have the following expression

$$\mathcal{V} = \frac{r_H^6 \Omega_H^2}{1 - r_H^2 \Omega_H^2}, \quad \mathcal{U} = -\frac{r_H^2}{1 - r_H^2 \Omega_H^2}, \quad \mathcal{W} = \frac{r_H^4 \Omega_H}{1 - r_H^2 \Omega_H^2}. \quad (3.26)$$

The  $d = 5$  MP black holes with equal-magnitude angular momenta emerge smoothly from the static Schwarzschild-Tangherlini black hole when the event horizon velocity  $\Omega_H$  is increased from zero. For a given event horizon radius, the solutions exist up to a maximal value of the horizon angular velocity  $\Omega_H^{(c)} = 1/\sqrt{2}r_H$  for which the black hole becomes extremal ( $T_H \rightarrow 0$ ). Expressed in terms of the mass-energy  $M$  and the equal-magnitude angular momenta  $|J_1| = |J_2| = J$ , this bound reads  $27\pi J^2/8G < M^2$ . The extremal solution saturating this bound has a regular but degenerate horizon.

<sup>1</sup>This metric is usually expressed in terms of the mass  $M$  and the angular momentum parameter  $a$ , with  $M = r_H^2/2(1 - r_H^2 \Omega_H^2)$  and  $a = r_H^2 \Omega_H$ .

### 3.2 Charged, non spinning black holes

In the absence of rotation, charged black holes exist generalizing the Reissner-Nordstrom solutions. The equations are considerably simpler since  $f(r) = b(r)$ ,  $h(r) = r^2$  and  $W(r) = A(r) = 0$  while the non trivial fields read

$$f(r) = 1 - \frac{2M}{r^2} + \frac{Q^2}{3r^4} \quad , \quad V(r) = V_0 + \frac{Q}{r^2} \quad , \quad M = \frac{r_H^2}{2} + \frac{Q^2}{6r_H^2} \quad (3.27)$$

These black holes exist for  $0 \leq Q^2 < 3r_H^4$  and becomes extremal in the limit  $Q^2 \rightarrow 3r_H^4$ .

## 4 Uncharged Hairy Black Holes

In the absence of the electromagnetic field, a family of hairy black holes exist on a specific domain of the  $r_H, \Omega_H$  parameter space. These solutions were obtained in [13] but we shortly discuss them again for completeness. The  $\Omega_H - M$  domain of these solutions is represented on Fig. 1 (left side) where a few values of  $r_H$  are supplemented. The solutions exist for  $0.924 < \Omega_H < 1$  in the region limited by boson stars (red line, reached in the limit  $r_H \rightarrow 0$ ) and by a family of singular extremal solutions (blue line:  $T_H = 0$ ). The intermediate constitutes the regular black holes. On the right side of Fig. 1 The domain of Myers-Perry and hairy black holes are superposed, demonstrating that both families of solutions are disjoint.

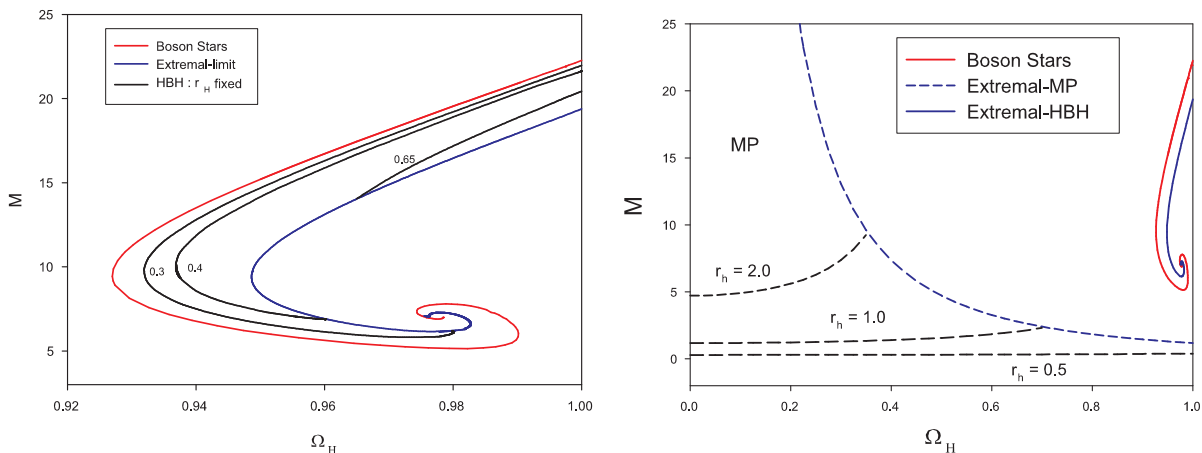


Figure 1: Left: Mass-frequency relation for boson star solutions (red line), for hairy black holes with three values of  $r_H = 0.3, 0.4, 0.65$  (black lines) and for extremal solutions (blue line). Right: Sketch of the domains of Myers-Perry and hairy black holes in the  $\Omega_H - M$  plane.

## 5 Charged-hairy-solutions

Any hairy black holes, e.g. any point of Fig. 1 (left side) characterized by a couple  $(r_H, \Omega_H)$  gets deformed in the presence of an electromagnetic field. The purpose of this section is to study the pattern of solutions in dependence of the gauge coupling  $q$ . Unlike the Myers-Perry solutions, the equations with the matter fields have no closed form solutions and have to be solved numerically. We used the numerical routine COLSYS [23] to perform the integration. The radial interval was discretized by means of a mesh of 300 points and the equations were solved with a relative error of less than  $10^{-6}$ .

The frequency of the scalar field  $\omega$  is fixed via the condition (2.18). Accordingly, synchronized solutions (that is with  $\omega = \Omega_H$ ) occur **iff**  $q = 0$  or  $A_H = 0$ . These cases will be discussed separately.

## 5.1 Synchronized solutions: Case $q = 0$

This case corresponds to the ungauged model, whose  $d = 4$  counterpart is studied in details in Sect. 2 of [19]. In the absence of a direct coupling of the scalar fields to the electromagnetic field (i.e. for  $q = 0$ ), the spinning solution gets deformed through a non-trivial magnetic potential  $A(r)$  through the influence of the rotating space-time. The parameter controlling the magnetic potential is  $A_H \equiv A(r_H)$ . The electromagnetic field vanishes identically for  $A_H = 0$  and becomes non trivial for  $A_H \neq 0$ . The effect is demonstrated on

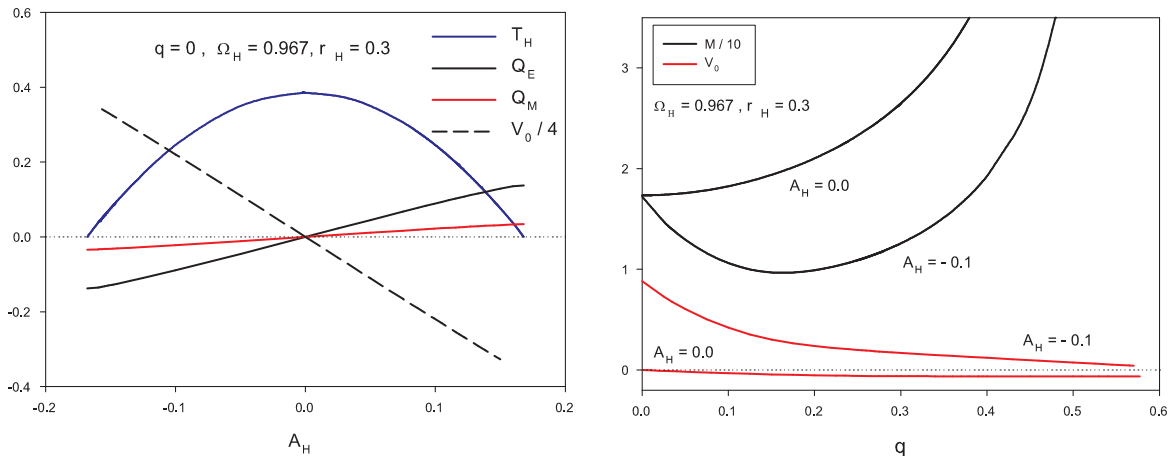


Figure 2: *Left:* Several quantities characterizing the black holes for  $q = 0$  as functions of the parameter  $A_H$ . *Right:* The mass  $M$  and electric potential  $V_0$  as function of  $q$  for the solutions corresponding to  $A_H = 0.0$  and  $A_H = -0.1$ .

Fig. 2 (left side) : the electric and magnetic parameters  $Q_e$ ,  $Q_m$  and the electric potential  $V_0 \equiv V(\infty)$  are reported as functions of  $A_H$ . The temperature  $T_H$  of the black hole is supplemented and reveals that a limiting configuration with zero temperature is approached for a maximal value of  $|A_H|$ . In the ungauged case, since  $q = 0$ , the equations simplify drastically. In particular they become symmetric under  $A_\mu \rightarrow -A_\mu$ , explaining the symmetry of Fig. 2 (left) under the sign reversal of  $A_H$ . The mass and angular momentum of these solutions depend weakly on  $A_H$  and have not been reported. The qualitative features of Fig. 2 seem to be generic, it was checked for a several values of the parameters  $r_H$  and  $\Omega_H$ .

## 5.2 Synchronized solutions : case $A_H = 0$

Synchronized black holes strongly coupled to the electromagnetic field are obtained by increasing gradually the gauge coupling parameter  $q$  while imposing  $A_H = 0$  as boundary condition. The electric potential  $V_0$  is negative and decreases monotonically while  $q$  increases; this is shown on the right side of Fig.2. Our numerical results strongly suggest that the effective squared mass  $\mu^2 - (\omega - qV_0)^2$  approaches zero for  $q \rightarrow q_{\max}$  (see Fig. 3 (left side)); as a consequence localized solution do not exist for  $q > q_{\max}$ . The value  $q_{\max}$  in fact corresponds to the value of the coupling constant for which the bound state condition (2.17) ceases to be satisfied. On the example of Fig. 3 , i.e. with  $r_H = 0.3, \Omega_H = 0.967$ , we find  $q_{\max} \approx 0.577$ . The temperature corresponding to this set of solutions has been reported on the right side of Fig. 3.

On Fig. 4 (left side) the effective energy density of the scalar part and vector part of the matter fields are reported for  $q = 0.0$  and  $q = 0.4$ . For  $q = 0$ , the energy density of the vector field is identically null. One can also see that the maximum of the scalar energy density is closer to the horizon in this case compared to the case  $q \neq 0$ . This might be interpreted as follows : The case  $q = 0$  correspond to a uncharged massive scalar field. In this case, the existence of bound state is insured by the gravitational interaction

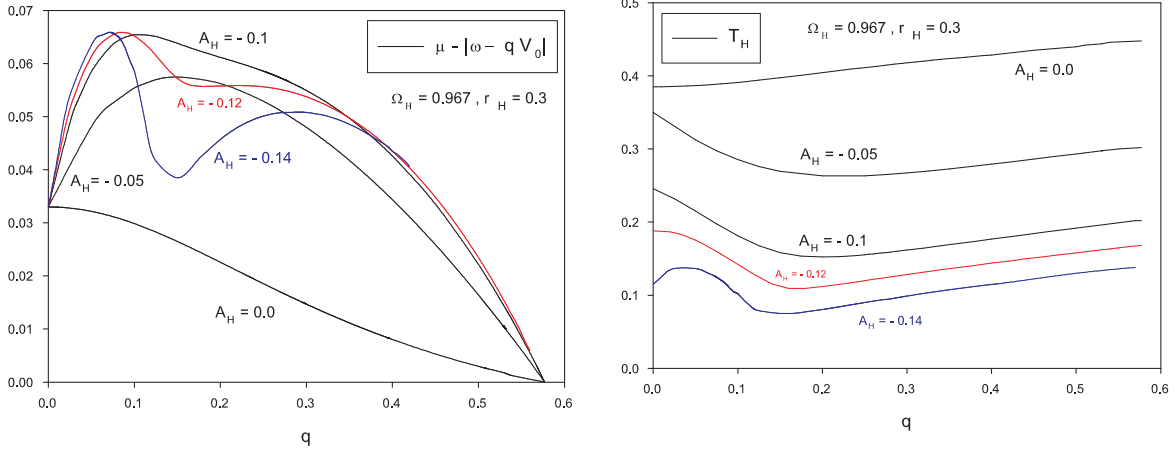


Figure 3: *Left*: The combination  $\mu - |\omega - qV_0|$  as function of  $q$  for several values of  $A_H \leq 0$ . *Right*: The Temperature for the same set of solutions.

and the scalar “cloud” is located at a given distance of the black hole horizon. In the case  $q \neq 0$  the scalar field is electrically charged, more precisely every quantum in the “cloud” acquire the same charge  $q$ , and then every quantum would electrically try to grow back each other so that the macroscopic scalar field (the position of the maximum) would be localized further away compared to the uncharged case. This qualitative argumentation can also explain the existence of  $q_{\max}$ . This correspond to the value of the scalar electric charge for which gravity cease to be strong enough to compensate for the electrostatic repulsion and guarantee a bound state.

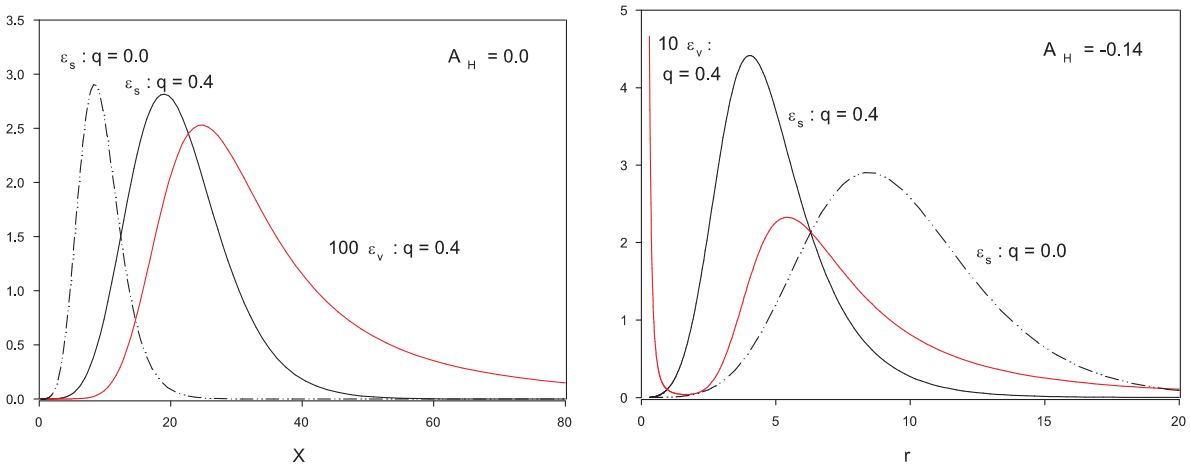


Figure 4: *Left*: The scalar (black) and vector (red) energy density for  $q = 0$  (dot-dashed) and for  $q = 0.4$  (solid) for  $A_H = 0$ . *Right*: Idem for  $A_H = -0.14$ . On both side the dot-dashed curve is the same allowing the reader to compare the plots. Both plots are realized for  $r_H = 0.3$  and  $\Omega_H = 0.967$ .

### 5.3 General case : $A_H \neq 0, q \neq 0$

In the general case, any uncharged hairy solution (with fixed  $r_H, \Omega_H$ ) lead to a two-parameter family of charged solutions characterized by the value  $A_H$  and the gauge coupling constant  $q$ . This domain of existence of the solutions is largely limited by the bound state condition (2.17).

Setting for definiteness  $A_H < 0$ , the numerical results indicate that the solutions stop to be localized for  $q > q_{\max}$ , i.e. when the effective frequency becomes imaginary. These results also strongly suggest that the value  $q_{\max}$  is independent of the value  $A_H$ . To illustrate this statement, the dependence on  $q$  of the quantity appearing in (2.17) is reported on Fig. 3 (left side) for several values of  $A_H \leq 0$ . The plot clearly suggest that the value  $q_{\max}$  is independent of  $A_H$ , although the curves are substantially different for the intermediate values of  $q$ . The temperature of these families of solutions are reported on the right side of Fig. 3.

For  $A_H > 0$ , the domain is considerably smaller because, due to the negative sign of  $V_0$ , the effective frequency quickly becomes imaginary. We did not study this case in details.

On Fig. 4 (right side) we report the effective energy density for the scalar part and vector part for  $A = -0.14$  and for  $q = 0.0$  and  $q = 0.4$ . Here, the maximum of the scalar energy density is closer to the horizon for  $q \neq 0$ . This behaviour remains true until  $q$  becomes close to  $q_{\max}$ . While approaching  $q_{\max}$  the maximum of the scalar energy density would become more and more distant from the horizon until the bound state condition stop to be satisfied.

The interpretation in this case is similar to the previous one : The case  $q = 0$  correspond to an uncharged scalar field as we already discussed. Here when  $q \neq 0$ , since  $A_H \neq 0$ , the system would be subject to electric and magnetic interaction since the black hole as both electric and magnetic charge. For a given value of  $A_H$  (and then for a fixed magnetic interaction with the black hole), on most of the allowed parameter space, the magnetic effect is dominant with respect to the electric repulsion. The effect of this magnetic interaction will be to concentrate the scalar field near the horizon. Nevertheless, if one continue to increase  $q$ , the electric repulsion will finally becomes dominant and lead to a dispersion of the scalar field. The interesting thing here is that this breakdown occur for a value of  $q$  independent of the parameter of the model, i.e. not only  $A_H$  but also  $\Omega_H$  and  $r_H$ . This ‘‘universality’’ of  $q_{\max}$  appears as a surprise and we did not found any physical or analytic explanation for it.

Let us finally mention that, when the value  $q_{\max}$  is approached, the mass and angular momentum of the black hole become very large and possibly tend to infinity (see Fig.2, right side). Due to numerical difficulties this statement can hardly be proven but an inspection of the profiles presented on Fig. 5 show that the fields have tendency to spread over space for  $q \rightarrow q_{\max}$ . We checked that this behaviour persist for different values of  $A_H, r_H$  and  $\Omega_H$  than the ones presented on the figure.

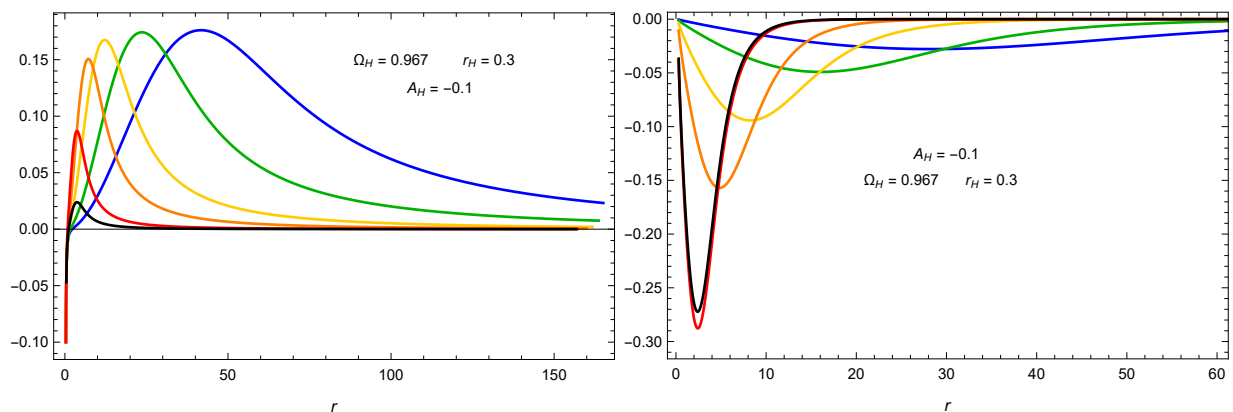


Figure 5: *Left*: Profile of the magnetic potential  $A$  with  $A_H = -0.1$  for  $q = 0.1, 0.3, 0.5, 0.55, 0.57$  and  $0.575 \approx q_{\max}$  respectively in black, red, orange, yellow, green and blue. These curves are for  $\Omega_H = 0.967$  and  $r_H = 0.3$ . *Right*: Idem for the scalar function  $F$ .

## 6 Conclusion

This paper is devoted to the study of higher dimensional rotating charged black holes in Einstein gravity supplemented by a doublet of complex massive scalar fields (see section 2 for the details of the model).

This model contains numerous parameters. Within our ansatz, once fixed the units ( $8\pi G = 1$  and  $\mu = 1$ , where  $\mu$  is the mass of the scalar doublet), the solutions are determined in terms of 4 parameters : the position of the event horizon  $r_H$ , the angular velocity of the black hole at the horizon  $\Omega_H$ , the gauge coupling parameter  $q$  and the value of the magnetic potential at the horizon  $A_H$ .

In sections 3 and 4 we reviewed the main results already available in the literature for the non hairy and uncharged hairy sub-sectors of our model.

In section 5 we finally come with new results for the most general cases *i.e.* charged rotating hairy solutions. We saw that, any uncharged hairy solution (described by  $r_H$  and  $\Omega_H$ ) gives rise to a two-parameter space of solutions (controlled by  $q$  and  $A_H$ ). As expected, the domain of existence for the solutions is asymmetric with respect to a change of sign of  $A_H$  only when  $q \neq 0$ . We saw that the domain of existence was more restricted for  $A_H > 0$  while for  $A_H < 0$  solutions might exist for a significantly higher value of  $|A_H|$ . In both cases, the bound in the domain is controlled by the condition limiting the possible existence of regular solutions with **localized** scalar field. That is  $\mu - |\omega - qV_0| > 0$ , where  $\omega$  is the harmonic frequency of the scalar doublet and  $V_0$  the value of the electric potential at infinity. Basically, this condition fixes the maximal value of the gauge coupling parameter, say  $q_{\max}$ , for which the presence of localized scalar field might be supported by the rotating charged black hole. Our numerical results tend to prove that this value  $q_{\max}$  is “universal”, by this we mean independent of  $A_H$ ,  $r_H$  and  $\Omega_H$ . In our units, we found  $q_{\max} \approx 0.577$ .

Finally, let us mention that the link between the harmonic frequency of the scalar doublet  $\omega$  and the angular velocity of the black hole at the horizon  $\Omega_H$  was also established and gives rise to the condition:  $\omega - \Omega_H + qA_H\Omega_H = 0$ . This condition generalizes the synchronization condition known for uncharged solutions.

## References

- [1] R. Emparan and H. S. Reall, Living Rev. Rel. **11** (2008) 6.
- [2] D. Lovelock, J.Math.Phys. **12** (1971) 498-501.
- [3] P. T. Chrusciel, J. Lopes Costa and M. Heusler, Living Rev. Rel. **15** (2012) 7.
- [4] R. Emparan and H. S. Reall, Phys. Rev. Lett. **88** (2002) 101101.
- [5] R. Ruffini and J. A. Wheeler, Phys. Today **24** (1971) no.1, 30.
- [6] H. Luckock and I. Moss, Phys. Lett. B **176**, 341 (1986).
- [7] J. D. Bekenstein, "Black hole hair: 25 - years after," In \*Moscow 1996, 2nd International A.D. Sakharov Conference on physics\* 216-219 [gr-qc/9605059].
- [8] C. A. R. Herdeiro and E. Radu, Phys. Rev. Lett. **112** (2014) 221101
- [9] C. Herdeiro and E. Radu, Phys. Rev. D **89** (2014) no.12, 124018
- [10] C. A. R. Herdeiro, E. Radu and H. F. Runarsson, Int. J. Mod. Phys. D **25** (2016) no.09, 1641014.
- [11] R. C. Myers and M. J. Perry, Annals Phys. **172** (1986) 304.
- [12] B. Hartmann, B. Kleihaus, J. Kunz and M. List, Phys. Rev. D **82** (2010) 084022.
- [13] Y. Brihaye, C. Herdeiro and E. Radu, Phys. Lett. B **739** (2014) 1
- [14] Y. Brihaye, C. Herdeiro and E. Radu, Phys. Lett. B **760** (2016) 279
- [15] O. J. C. Dias, G. T. Horowitz and J. E. Santos, JHEP **1107** (2011) 115
- [16] S. Hod, Phys. Lett. B **755** (2016) 177.
- [17] S. Hod, Phys. Lett. B **751** (2015) 177
- [18] S. Hod, Phys. Lett. B **713** (2012) 505
- [19] J. F. M. Delgado, C. A. R. Herdeiro, E. Radu and H. Runarsson, Phys. Lett. B **761** (2016) 234
- [20] N. Grandi and I. Salazar Landea, Phys. Rev. D **97** (2018) no.4, 044042.
- [21] Y. Brihaye and B. Hartmann, "Critical phenomena of charged Einstein-Gauss-Bonnet black holes with charged scalar hair," arXiv:1804.10536 [gr-qc]; Class. Quant. Grav. (in press).
- [22] Y. Brihaye, T. Delplace, C. Herdeiro and E. Radu, Phys. Lett. B **782** (2018) 124.
- [23] U. Ascher, J. Christiansen, R. D. Russell, Math. of Comp. **33** (1979) 659;  
U. Ascher, J. Christiansen, R. D. Russell, ACM Trans. **7** (1981) 209.